Highly Integrated Power Module for PV and Storage iPV++

Angelica Becker, Jeffrey Claudio and Emmanuel Ortiz

College of Engineering and Computer Science, University of Central Florida, Orlando, Florida, 32826-2450, USA

***Abstract* — As photovoltaic systems become more readily available to society, the demand for these systems have increased. This paper presents the research and design of a highly integrated power module. The multiple components are as follows: (1) DC/DC converter; (2) DC/AC inverter; (3) Solar Panel.**

***Index Terms* — Battery, DC/AC Power Converter, DC/DC Power Converter, Solar Energy.**

I. Introduction

According to SEIA, "Solar energy is the cleanest and most abundant renewable energy source available, and the U.S. has some of the richest solar resources in the world". As we know, the sun is virtually an unlimited energy source and there are various ways to harvest this energy. Methods of harvesting consist of using photovoltaic cells, solar thermal collectors, solar concentration centers with mirrors, and passive solar designs.

Starting with photovoltaic cells, they are able to convert solar rays into energy. "When sunlight hits a cell, the energy knocks electrons free of their atoms thus allowing them to flow through the material. The resulting DC (direct current) electricity is then sent to a power inverter for conversion to AC (alternating current), which is the form in which electric power is delivered to homes and businesses" [1].

Our senior design project takes the average solar panel system and converts it into a single package, a modern photovoltaic system. A photovoltaic panel, battery, and inverter all three combined into one product that is intertwined within the power grid. "The main goal of this proposed project is to investigate, design and develop an advanced integrated and cost-effective technology consisting of PV, smart inverter, and battery management".

II. Overview iPV++

The main goal for this project is to create an integrated power module for the solar panels that include the microinverter, DC/DC converter, microcontroller and battery pack. This new power module will have to be small enough to fit behind the individual solar panels and have a detachable battery to accommodate different battery size requirements. This new module will also have to be easily installable that way people can buy them and install it themselves. When designing the DC/DC converter, we have make sure it's at least 95% efficient to be able to compete with other DC/DC converters already in the market.

Another goal is to create an algorithm to program into the microcontroller that will be able to control the different modes of operation for the converter such as the solar panel charging the batteries and delivering power to the load, or both the battery and solar panel supplying power. Figures 1-3 show the general design of the finalized product.

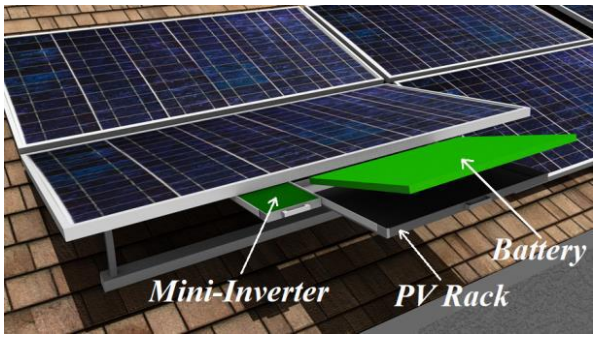

Fig. 1. Lift and Sliding Mechanism.

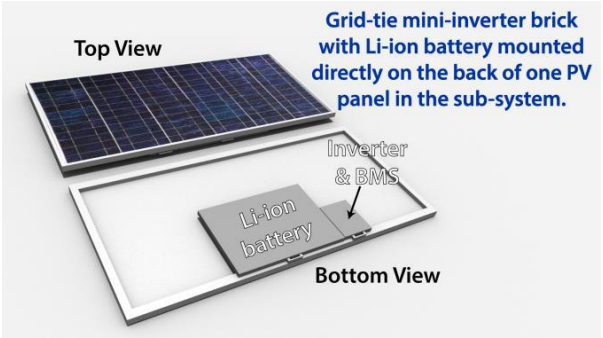

Fig. 2. iPV++ Module.

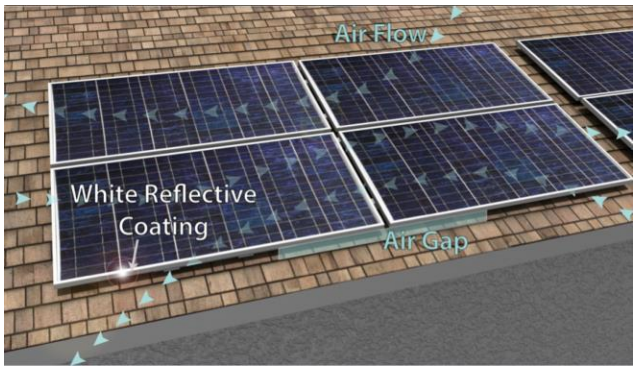

Fig. 3. Standard Configuration of iPV++.

While working in conjunction with the mechanical engineering team, the proposed system will be built to fit under a solar panel. It will also have a racking system built by the mechanical engineering team that will have a lifting and sliding mechanism and will contain the iPV++ integrated power module and an interchangeable battery pack. The battery size will be optimized in regards to how much solar power can be generated in a given area. Since the racking system is going to allow components to be separated, this will increase the ease of use to allow customers to install the module themselves.

The components that are going to be used will have to be able to withstand a wide temperature range -20°C to 70°C (-4°F to 158°F) and need to be in a weatherproof sealed containment unit to withstand rain, snow, and other types of environmental harm. The connection between the battery and the iPV++ power module will have to be a sealed quick connect to allow for fast installation or replacement of the battery.

III. DC/DC Converter

The DC/DC converter is the main part of this project. The goal is to create a dual input DC/DC converter that will have a battery connected on one side as an input and output and the solar panel on the other side only as an input. This converter will be designed to have two modes of operation. The first mode is configured to charge the battery and provide power to the load and the second mode utilizes both the solar panel and battery to deliver maximum power to the load. Lastly, this converter must incorporate a boost converter to be able to boost the voltage from the solar panels and have enough current to charge the battery.

The boost converter is a circuit designed to step up the voltage when the input does not have enough voltage. The primary component used in boosting the voltage at the output is the inductor. When the switch is closed, the voltage source charges the inductor as the switch acts like a short to ground. When the switch is opened, the energy stored in the inductor creates a high voltage spike in series with the voltage source thus charging the battery [2].

For the purposes of this project, we will be looking at a special variant of the boost converter proposed by our sponsor known as the dual-input LLC resonant converter. There are many stages in the conversion process of the inputs where the first stage consists of a switch network. Shown in Fig. 4 is the diagram of the proposed converter where the switches are represented as mosfets.

The MOSFET transistor acts as a switch when the gate and source are biased to their threshold voltage thus shorting the path between the drain and source. When switches S_1 and S_4 are shorted and the other two are opened, the solar panel is generating current in one direction. When switches S_2 and S_3 are shorted and the other two are opened, the batteries are generating current in the opposite direction. When this process is repeated, the inputs are acting as an AC signal with the frequency dependent on the microcontroller.

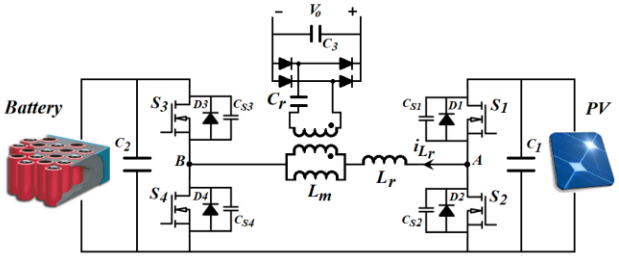

Fig. 4. DC-DC Converter.

Continuing the discussion of the modes of operation, the first mode is configured for both charging the battery and delivering power to the load. Referring to Fig. 4, the configuration for this mode has the switches S_1 shorted, S_2 opened, and S_3 and S_4 alternating. What allows this mode to charge the battery is the inductor L_r because the topology of the current configuration mimics that of a boost converter. In this topology when S_4 is shorted and S_3 is opened, energy is being stored in the inductor L_r. When the switches S4 is opened and S_3 is shorted, the energy stored in the inductor combines with the energy coming from the solar panel to boost the voltage to charge the battery. Since this is happening continuously, the current is alternating thus also providing power to the opposite side of the transformer to deliver to the load.

The other feature that this mode will offer is control of how much power is being used to charge the battery and deliver to the load. A simulation was done on LTspice to show the behavior of this feature. Ideally the output voltage of the converter should be consistently around 400 V no matter what load is placed. By changing the switching frequency of the power mosfets, the voltage

across the load can stay localized around its nominal value. As shown in Fig. 5, the frequency is not a linear relationship with respect to power. Despite this complication, this will be controlled by a microcontroller by using voltage sensing at the output to control the switching frequency to provide 400 V at the output.

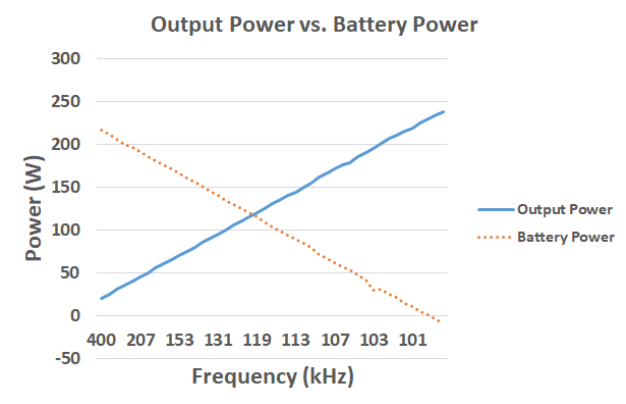

Fig. 5. Frequency Manipulation.

The other mode of operation is strictly to provide power to the load. As explained before, when switches S_1 and S_4 are shorted and the other two are opened, the solar panel is generating current in one direction. When switches S_2 and S_3 are shorted and the other two are opened, the batteries are generating current in the opposite direction. This allows all power from the solar panel and battery to go directly to the load.

Besides being able to supply more power to the load, this mode has a feature that allows how much power is being outputted by either source with phase shift control. Before going into further explanation, S_2 is always the inverse of S_1 and S_4 is always the inverse of S_3. When applying a phase shift of one degree, depending on the orientation, there will be a moment in time where S_1 and S_3 are both on or S_2 and S_4 are both on. By adding positive phase shift, the solar panel will output less power and the battery will output more power. When the phase shift is negative, the opposite effect occurs. Fig. 6 shows the power distribution with respect to phase shift. Comparing the axes, the relationship between phase shift and power is linear which will allow programming the microcontroller to be much easier as opposed to the frequency control.

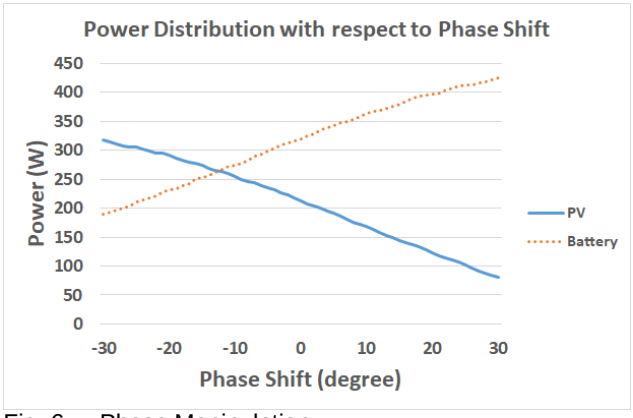

Fig. 6. Phase Manipulation.

A. DC/DC Converter Parts Selection

For the converter many parts had to be carefully selected to build a robust and reliable system. The power MOSFETS were the first thing to consider since they would be the most active components in the first stage of the converter. By running simulations on LTspice and testing the two modes of operations, the voltage between the drain and source peaked around 60 V. This meant we had to choose transistors that were rated for a voltage higher than the nominal values. Another factor in choosing the MOSFETS was the turn on resistance of the transistor. When the switches are shorted, there is still resistance between the drain and source of the MOSFET and the lower the resistance, the more power efficient the transistors are. Aside from these parameters, the voltage required to turn on the transistor was also another factor to consider. Depending on the size and type of transistor, the gate to source voltage will also vary. In the case with power MOSFETS, the voltage required to switch on the transistor is around 10 V. To meet the requirements for the given parameters, the IPB020N10N5ATMA1 from Infineon Technologies was chosen. Shown in Tbl. 1 are the device parameters for the given device.

FET Type	N-Channel

Drain to Source Voltage (Vdss)	100V
Current - Continuous Drain (Id) @ 25°C	120A
Drive Voltage (Max Rds On, Min Rds On)	6V, 10V
Rds On (Max) @ Id, Vgs	2mΩ @ 100A, 10V
Vgs (Max)	± 20V
Operating Temperature	-55°C ~ 175°C

Tbl. 1. Device Parameters for the IPB020N10N5ATMA1.

Since the power MOSFETS requires 10 V to activate which is too high for the microcontroller to output, a gate driver is required. A gate driver a type of power amplifier that takes a low voltage input and amplifies it to a higher voltage to activate transistors. For the first stage in the converter since there are four power MOSFETS, there would be a need for four PWM signals coming from the microcontroller. To simplify the design, since each pair of switches are related by their inverse, only two PWM signals would be required. Since only two signals are going to be outputted by the microcontroller, a gate driver with two outputs would be required. When one of the outputs activates one transistor, the other output would deactivate the other transistor.

Choosing the gate driver to use for this design was not too difficult due to the parameters required. First it had to be designed for high frequency applications and had to output around 10 V to turn on the power MOSFETS. For these reasons the MIC4103YM from Microchip Technology was chosen. Tbl. 2 shows the device parameters for the selected gate driver.

Gate Type	N-Channel MOSFET
Driven Configuration	Half-Bridge
Voltage - Supply	9V ~ 16V
Rise / Fall Time (Typ)	10ns, 6ns
Operating Temperature	-40°C ~ 125°C

Tbl. 2. Device Parameters for the MIC4103YM.

As shown in Tbl. 2 the rise / fall time is in the range of nanoseconds which satisfies high frequency switching for the power MOSFETS.

For the DC/DC converter, it was decided that the STM32F334K8T7 would be used. This microcontroller has the following parameters:

STM32F334K8T7	
I/O	10
Main Memory	64KB
Clock Speed	72 MHz
PWM	20
Advanced Timer	4 Independent Channels

Tbl. 3. Device Parameters for the STM32F334K8T7.

B. Component Design for the DC/DC Converter

In lieu of ordering the transformer and inductor for the DC/DC converter, it was required to build these components from scratch. Using a coil former, wire and inductive core, we designed the components to meet our specifications.

IV. DC/AC INVERTER

According to our sponsor, our group was given free reign over which inverter topology was to be chosen for our design. One of the most important considerations in the final design implementation and overall operation is the ability to reach high levels of efficiency with respect to power output for multiple power configurations.

Similar to the square wave inverter, the pure sine wave inverter outputs a sine wave when the input is a DC source. The project requires the inverter to output a 120 V_{RMS} sine wave at 60 Hz. A basic sine wave inverter has a similar topology to the square wave inverter except that it has a low-pass filter at the output. Another difference about this type of inverter is that the switching frequency is dependent on pulse width modulation. This controls how long the switches stay on and what controls this is the reference sinusoidal signal.

A. Sinusoidal Pulse Width Modulation

In order to output a sinusoidal wave, it was decided to use sinusoidal pulse width modulation (SPWM). SPWM works by using a reference sinusoidal waveform and comparing it to a triangular waveform to modulate the width of the pulse width signal. The width of the pulse width signal is changed in accordance to the amplitude of the sine wave.

Shown in Fig. 7 are three signals that represent the SPWM. SPWM can be implemented through an analog circuit; however, it can also be implemented digitally. The microcontroller for the inverter stage will output the PWM signal to the power mosfets to generate a waveform similar to the square pulses in Fig. 7 .

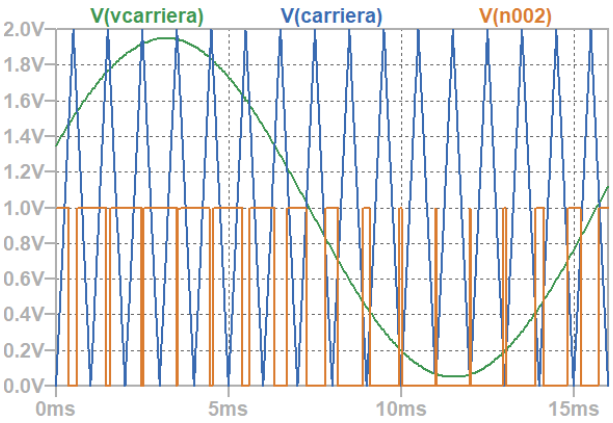

Fig. 7. SPWM Signal. V(vcarriera) is the reference sine signal, V(carriera) is the triangle signal, and V(n002) is the SPWM signal.

B. LC Filter

To ensure a smooth signal from the output of the inverter, an LC filter was added to the inverter. The reason a filter is needed is to filter out the harmonics of the pulsed square waves. A sine wave usually has a large harmonic in the frequency domain corresponding to its operating frequency. The values of the components were calculated using the following equations:

$$f = \sqrt{f_s \times f_r} \tag{1}$$

$$L = \frac{1}{4C(\pi f)^2}. \tag{2}$$

(1) uses the switching frequency f_s and the reference sine wave frequency (f_r = 60 Hz) to give the variable f that is used in (2) to calculate the values for the LC filter. When the switching frequency increases, the value selected for inductor will also decrease making component selection much more feasible. Using these equations, a spreadsheet was created that varies the switching frequency at a given capacitance to find an inductor value as shown in Fig. 8. The values that were chosen for the capacitor was 6 uF and the inductor had a value of 470 uH. These values were configured for a switching frequency around 150 kHz. Shown below in Fig. 9 is a plot of the filtered sine wave and the SPWM signal.

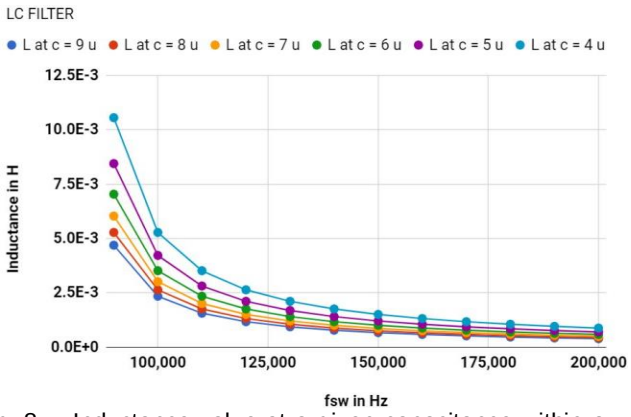

Fig. 8. Inductance value at a given capacitance within a range of switching frequencies.

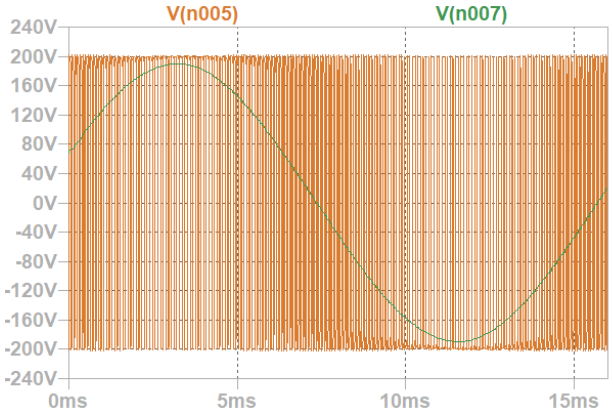

Fig. 9. Inverter Output. V(n005) is SPWM signal and V(n007) is the filtered sine wave.

C. DC/AC Inverter Parts Selection

The inverter topology selected for the inverter design is the half-bridge. This topology was selected because it is a simpler design and is more cost effective than a full-bridge inverter. For the parts selection of the inverter stage, power MOSFETS were also required. The half-bridge topology involves two MOSFETS and for the inverter stage since the voltage is going to be much larger from the DC link, we need them rated for over 400 V and have a low switching loss since we are going to be using high frequencies to perform SPWM. To meet these requirements, a spreadsheet was created to calculate the total power losses using the following equations with the values found in the datasheets.

$$Conduction\ Losses\ (L_c) = R_{dsONhot} \times {I_{in}}^2 \quad (3)$$

$$Switching\ Losses\ (L_s) = I_{in} \times f_s \times T_f \quad (4)$$

$$Gate\ Charge\ Losses\ (L_q) = 2 \times V_{gs} \times Q_g \times f_s \quad (5)$$

$$Total\ Losses = L_c + L_s + L_q. \quad (6)$$

Where R_{dsON} is the internal resistance, I_{in} is the input current, f_s is the switching frequency, T_f is the fall time, and Q_g is the total gate charge. This information was used to create Fig. 10 and Fig. 11 to aid in the selection of the best MOSFET. The MOSFET chosen for the inverter stage was the IPB60R080P7ATMA1 from Infineon Technologies. Tbl. 4 shows the device parameters for the selected device.

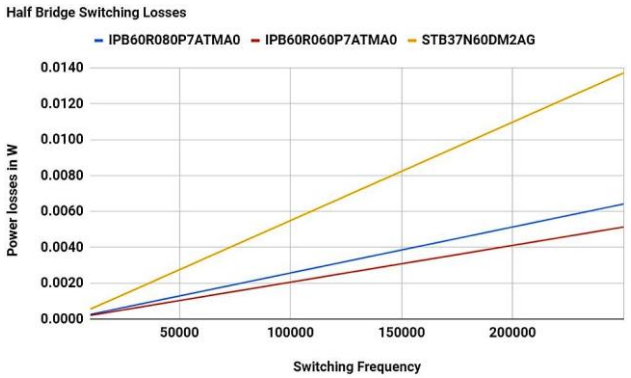

Fig. 10. Comparison of Switching Losses.

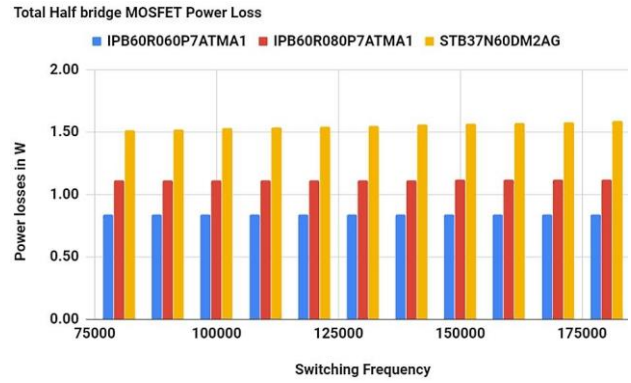

Fig. 11. Comparison of Total Power Losses.

FET Type	N-Channel
Drain to Source Voltage (Vdss)	650V
Current - Continuous Drain (Id) @ 25°C	37A
Drive Voltage (Max Rds On, Min Rds On)	10V
Rds On (Max) @ Id, Vgs	80mΩ @ 11.8A, 10V
Vgs (Max)	± 20V
Operating Temperature	-55°C ~ 150°C

Tbl. 4. Device Parameters for the IPB60R080P7ATMA1.

Looking at Tbl. 4 it is shown that the turn on resistance is 80 mΩ. This is much higher than the MOSFETS for the converter stage and that is because when the voltage rating of the MOSFET increases, the drain to source resistance also increases.

The next part that was essential for this design is another gate driver. Similar to the one in the converter stage, it will be used to activate the power MOSFETS; however, the voltage across the MOSFETS in the inverter stage are much higher reaching up to around 400 V. If regular gate drivers are used, there is a chance that the high voltage could travel to the microcontroller and damage the device permanently. To compensate for this issue, optocouplers are recommended for high voltage isolation. Similar to the converter stage, the desired optocoupler will be rated for high frequencies and have to handle over 400 V. To meet these design requirements, the HCPL-3180-300E from Broadcom Limited was chosen. Tbl. 5 shows the device parameters for the selected gate driver.

Technology	Optical Coupling
Voltage - Isolation	3750 Vrms
Voltage - Supply	10V ~ 20V
Rise / Fall Time (Typ)	25ns, 25ns
Operating Temperature	-40°C ~ 100°C

Tbl. 5. Device Parameters for the HCPL-3180-300E.

As for the microcontroller, the dsPIC33FJ16GS504 from Microchip was chosen. The original design required multiple pins to be used for sensing since the inverter was going to be connected to the grid. Due to time constraints,

the design had to be changed and the dsPIC33FJ16GS504 was still used for the design since everything was configured for the initial design.

V. Solar Panel

As the foundation of the project, photovoltaic cells convert solar energy into electrical energy through the photoelectric effect. The photoelectric effect essentially states that when photons strike the surface of certain materials, electrons would use this energy to break free [3]. This is a useful property and when implemented onto a semiconductor doped with electron and holes, the electrons would flow in one direction due to the internal electric field in the semiconductor. If used in a closed circuit, this would lead to current flow along with a small voltage. Since the voltage is usually too low to serve any practical use, these photovoltaic cells (or simply solar cells) are connected in series to raise the voltage thus increasing power output.

The types offered today are monocrystalline silicon, polycrystalline silicon, thin film (TFSE), amorphous silicon (a-Si), copper indium gallium selenide (CIS), building integrated (BIPV) and cadmium telluride (CdTe). A consolidated chart from the referenced website is offered in Tbl. 6.

Crystalline			
Advantages	Monocrystalline	Polycrystalline	Spring Ribbon
Efficiency %	Best (15-20%)	13-16%	13–14%
Small	Yes 4x thin film	No	Worst
Affordability	Least	No	No
Maintainability	Lower	Lower	Lower
Life Span	Best	Good	Good
Low Light	Best	Good	Good
Product Waste	A Lot of Waste	< Mono	> Mono
Manufacturing Cost	< Polycrystalline	Low	Very high
Other	If dirty, entire circuit could break down	Heat brings efficiency down	Heat brings efficiency down
Attractive	More	Less	Less

Tbl. 6. Comparison Table of Solar Panels.

With an efficiency of 13-16%, polycrystalline based panels are also based of silicon but are made of fragmented crystals oriented in many shapes and sizes. Each section in the fragmented structure is differentiated by grain sizes which control the performance of how the solar cells will perform [4]. A larger grain size leads to greater efficiency and reduced combination in the depletion region of a P-N junction [5].

Due to limited availability and funds, we chose to go with a 38.5” x 77” 72 cell Canadian Solar polycrystalline panel. This panel will be connected to the DC/DC converter to supply power to the battery and any load that is connected.

Canadian Solar Polycrystalline Panel	
Nominal Maximum Power	310 W
Optimum Operating Voltage	36.4 V
Optimum Operating Current	8.52 A
Open Circuit Voltage	44.9 V
Short Circuit Current	9.08 A
Maximum Series Fuse Rating	15 A

Tbl. 7. Device Parameters for Canadian Solar Polycrystalline Panel.

VI. Battery

The second input into the iPV++ module will be the battery. The battery will be used to store the energy locally on each solar panel instead of a battery bank inside of the house. This battery will also provide energy into the grid dependent on how much power the iPV++ module has decided to send into the load from the battery. The battery used for the project will have to be weatherproof and be able to withstand high temperatures.

The system requires a 40 V, 250 W lithium-ion cobalt battery. Lithium-ion cobalt batteries are made from lithium carbonate and cobalt. They have very high capacity and are used in small electronics. Our battery will be supplied by AllCell. The size of the battery will be calculated depending on how much solar radiation is available for the solar panel to convert into electricity.

VII. Mechanical Design

The frame design was modeled based on the frames in today’s market; however, we intended to allow more

flexibility in working with various components of the panel while conserving parts and space. A quality comparison was made for different aspects of the frame, such as material, components, and structure. The frame material we chose to go with was aluminum because of the weight and cost savings, which outweighed the durability of a steel structure.

As far as the structure design, a rigid structure, a non-assisted rotating structure, similar to a pin and joint, and a piston or spring driven rotating structure were all considered. The flexibility and cost savings of a pin and joint type system proved to be a better choice than the others.

The components considered included a fan to conduct cooling on components such as the battery, the panel, and the circuit board. We decided that the battery was the highest heat producing component and with a 65ºC limit for the components. We also decided that with enough space between the components, natural convection carried enough heat to keep the temperature below critical levels. The space used is about 2 cm. which was more than enough space when calculated in our SolidWorks model.

IX. Conclusion

During this project, we have come to learn many things about power electronics and all of the research and time needed to come up with various designs. Part selection and PCB design have been both a challenging and interesting learning process.

In addition to this, during both semesters we have gained a substantial amount of knowledge of DC/DC converters, DC/AC inverters and PV systems. Moreover, having the opportunity to work on a multidisciplinary project has allowed us to gain real world experience by communicating thoughts and ideas to different branches of engineering.

Acknowledgement

The authors wish to acknowledge the assistance and support of Dr. Richie, Dr. Wei, Dr. Batarseh and the with the guidance throughout our project. We appreciate the time and patience that was required throughout the two semesters of senior design.

Biography

Angelica Becker is currently a senior at the University of Central Florida. She plans to graduate with her Bachelor of Science in Electrical Engineering in August 2018. She plans on working within the power systems field.

Jeffrey Claudio is currently a senior at the University of Central Florida. He plans to graduate with his Bachelor of Science in Electrical Engineering in August 2018 and to attend graduate school as soon as he finds a career.

Emmanuel Ortiz is currently a senior at the University of Central Florida. He plans to graduate with his Bachelor of Science in Electrical Engineering in August 2018.

References

[1] "About Solar Energy."SEIA, www.seia.org/initiatives/about-solar-energy.

[2] "Copper Indium Gallium Diselenide Solar Cells." Copper Indium Gallium Diselenide Solar Cells | Photovoltaic Research | NREL, www.nrel.gov/pv/copper-indium-gallium-diselenide-solar-cells.html.

[3] Knier, Gil. "How do Photovoltaics Work?" NASA, NASA, 6 Aug. 2008, science.nasa.gov/science-news/science-at-nasa/2002/solarcells.

[4] Kumar, P. (2016). Organic Solar Cells. Boca Raton: CRC Press.

[5] William Harris "How Thin-film Solar Cells Work" 7 April 2008. HowStuffWorks.com.<https://science.howstuffworks.com/environmental/green-science/thin-film-solar-cell.htm> 15 March 2018